

See discussions, stats, and author profiles for this publication at: <https://www.researchgate.net/publication/316070858>

# Electrospinning window: solution properties for uniform fibres from electrospinnable biopolymers

Conference Paper · January 2017

CITATIONS

0

READS

112

6 authors, including:



**Deborah Le Corre-Bordes**

Plant and Food Research

31 PUBLICATIONS 780 CITATIONS

SEE PROFILE



**Nick Tucker**

University of Lincoln

82 PUBLICATIONS 527 CITATIONS

SEE PROFILE



**Tim Huber**

University of Canterbury

24 PUBLICATIONS 381 CITATIONS

SEE PROFILE



**Mark Peter Staiger**

University of Canterbury

110 PUBLICATIONS 5,614 CITATIONS

SEE PROFILE

Some of the authors of this publication are also working on these related projects:



biomaterials electrospinning [View project](#)



All-cellulose composites [View project](#)

## **“Electrospinning window”: solution properties for uniform fibres from electrospinnable biopolymers**

**Deborah Le Corre-Bordes**

The New Zealand Institute for Plant & Food Research Limited  
Plant & Food Research, Private Bag 4704, Christchurch Mail Centre, Christchurch,  
8140, New Zealand

**Kathleen Hofman**

The New Zealand Institute for Plant & Food Research Limited  
Plant & Food Research Nelson, Box 5114, Port Nelson, Nelson, 7043, New  
Zealand

**Nicolas Bordes**

The New Zealand Institute for Plant & Food Research Limited  
Plant & Food Research, Private Bag 4704, Christchurch Mail Centre, Christchurch,  
8140, New Zealand

**Nick Tucker**

University of Lincoln, Brayford Pool, Lincoln, Lincolnshire, LN6 7TS, United  
Kingdom

**Tim Huber**

Department of Mechanical Engineering, University of Canterbury, Private Bag 4800,  
Christchurch, New Zealand

**Mark P. Staiger**

Department of Mechanical Engineering, University of Canterbury, Private Bag 4800,  
Christchurch, New Zealand

### **Abstract**

Electrospinning is a well-known method for producing continuous polymeric fibres with diameters in the submicron to nanometer range. In spite of the plethora of literature on the topic, the prediction of the morphology and/or topology of electrospun fibres remains a largely unresolved research topic due to the complex array of interacting parameters. The influence of various polymer solution properties including surface tension, conductivity and viscosity needs to be considered simultaneously although these measurements are rarely performed in a single study. In this study, the physical properties of aqueous poly(vinyl alcohol) solutions were obtained and compared with literature data for the purpose of defining target values. These newly defined target values were then verified using denatured whole chain marine collagen electrospun from two acids. This “electrospinning window” provides an informative resource for tissue engineering research studies.

### Introduction

Electrospinning is a dry spinning process that uses electrostatic force to draw fibres from a liquid polymer solution or a polymer melt and has a long history [1] of use for manufacturing submicron fibres. The process of fibre formation from the liquid is entirely physical, either by loss of solvent or freezing of a melt. The process has recently achieved widespread popularity in the laboratory as a method for the manufacture of polymeric fibres with diameters in the submicron to nanometre range [2].

Typically, electrospun fibres are formed by feeding the polymer solution through a thin capillary (aka nozzle or spinneret) that is held at high electric potential and placing the capillary close to a nearby grounded “collector” electrode. The application of an electric field acts to stretch the polymer solution such that the solution either breaks up into droplets or forms a narrow jet. The transition from electrospraying of droplets to electrospinning of fibres is dependent on the surface tension and viscoelasticity of the solution that acts to oppose the electrostatic forces. The balance of forces acting on the polymer solution is controlled by the interaction between viscoelastic properties, conductivity and surface tension of the solution. During electrospinning, initially the jet has a linear trajectory although after a small distance (~0.5–24 cm) from the capillary it begins to bend chaotically, entering a regime known as the whipping instability. The lower the viscoelastic properties of the polymer, the sooner the whipping motion will occur, and the higher the viscoelastic properties, the longer the straight jet distance will be, so that for melts the whipping instability is not observed.

The influence of various polymer solution parameters including surface tension, conductivity and viscosity need to be considered simultaneously although these measurements are rarely performed in a single study. The majority of studies have focussed on the “minimum” conditions required of the solution to ensure electrospinnability.

Polyvinyl alcohols (aka PVOH) are water-soluble, biocompatible synthetic polymers used since the early 1930s in a wide range of industrial, commercial, medical and food applications as resins, lacquers, surgical threads and food-contact applications [3]. PVOH is widely used for electrospinning as it easily renders nanofibres from aqueous solutions. However, there appears to be a lack of data on the physical properties of aqueous solutions of PVOH at concentrations of relevance to electrospinning [4]. In the present study, the aqueous solution properties (conductivity, surface tension and viscosity) of partially hydrolyzed PVOH ( $M_w = 118\text{kDa}$ ) were measured for concentrations up to 30 wt% PVOH. The resulting size and morphology of the electrospun fibres was examined. The physical properties of aqueous poly(vinyl alcohol) solutions obtained in this study were compared with data from the literature for the purpose of defining target values and to propose an “electrospinning window”. These newly defined target values were then verified using marine denatured whole chain (DWC) collagen as the spinning polymer.

### Experimental section

#### Materials

PVOH with an average molecular weight of  $118,000 \text{ gmol}^{-1}$  and degree of hydrolysis (HD) in the range of 85–90% was obtained from BDH Chemicals. Marine collagen in the form of denatured whole chains [5] was obtained from the Plant & Food Research BioProcessing Laboratory (BPL) in Nelson. Glacial acetic acid was purchased from Thermofisher, NZ. Citric acid monohydrate was purchased from Fisher Scientific, UK. Distilled water was used throughout the study.

#### Preparation of solutions

PVOH polymer solutions were prepared by dissolving portions of 1–2 g of PVOH granules in cold distilled water. The solutions were then heated in covered beakers for ~2 h in a water bath at 80–90°C with constant stirring at 200–300 rev/min to complete the solubilisation while minimizing water evaporation. The beakers were then removed from the water bath, sealed and allowed to cool in ambient conditions. Two drops of chloroform were added to the cooled solutions to avoid microbial growth and they were then stirred for 120 s at 400–500 rev/min. The final polymer concentration in each was determined by drying a small sample in a convection oven at 80°C. The polymer solution concentrations were not adjusted to targeted concentrations to ensure homogeneity of the solution. The solutions were conditioned at 25°C for 24–48 h prior to use.

The denatured whole chain collagen (DWCC) solutions were prepared by adding the freeze-dried collagen to the calculated amount of distilled water and acid. The samples were mixed and left to sit on the bench of a temperature-controlled room (20°C) for 1–2 h. A recent study by our group [6] has shown that for DWCC, electrospinning was not affected by a maturation time up to 18 h.

#### Characterisation of the solutions

The conductivity of the solutions was measured with a calibrated conductivity meter that has an integrated temperature sensor (Cyberscan PC510, Eutech Instruments, Singapore). Conductivity measurements were performed in triplicate.

The surface tension of PVOH was measured at 25°C using the Pendant Drop Method with an optical surface tension/contact angle meter equipped with a high-speed camera (CAM 200, KSV Instruments Ltd, Finland). Calibration was performed with distilled water stored at the same temperature prior to each measurement. The solutions were placed in a 1 mL syringe that was fitted with a new 1.27 mm diameter needle for each new measurement. Measurements were performed on the largest volume possible under hydrodynamic and mechanical equilibrium (i.e. before the droplet breaks). Image analysis was used to measure the drop shape factor ( $\beta$ ) and the radius of the drop curvature ( $R$ ), which together with the measured density compared to density of the the air interface ( $\Delta\rho$ ) and the gravitational

constant ( $g$ ), were used to calculate the surface tension:

$$\gamma = \frac{\Delta\rho \cdot g \cdot R^2}{\beta} \quad \text{Eq. 1.}$$

Average values were based on 10 replicates.

For collagen solutions, surface tension was measured using a SKZ1013A surface tension meter (SK2 Industrial, China) fitted with a Wilhelmy plate. Before each measurement the Wilhelmy plate was cleaned with distilled water and burnt using an alcohol lamp to remove any impurities. About 15–20 mL of sample was poured into a petri dish placed below the Wilhelmy plate. The plate was lowered to touch the surface of the liquid sample at which point the sample exerted a tension on the plate, which was recorded once the value had stabilised. For each solution, measurements were repeated 3 times and averaged.

The dynamic viscosity of each solution was measured using a rotational rheometer (Anton Paar MCR 301 Series, Australia) fitted with a cone-plate geometry of 50 mm in diameter,  $1^\circ$  angle (CP50-1) and a gap of 0.102 mm. The temperature was kept constant at  $20^\circ\text{C}$  using a Peltier hood. For all shear viscosity ( $\eta$ ) measurements the same procedure was followed. First the sample was pre-sheared at  $1 \text{ s}^{-1}$  for 3 min to homogenise and then allowed to relax for 2 min. For comparison purposes, we have reported the apparent dynamic viscosity at  $10 \text{ s}^{-1}$ .

### Electrospinning and characterisation of electrospun fibres

The solutions were electrospun using a Model ES4 electrospinning machine from Electrospinz Ltd (New Zealand). The solutions were supplied to the capillary via a gravity feed system. The PVOH solutions were electrospun at a potential difference of 15 kV and capillary-collector distance of 7 cm. The collagen solutions were electrospun at a working distance of 10 cm, the applied voltage was 30 kV and the fibres were collected on SEM pins for 10 s.

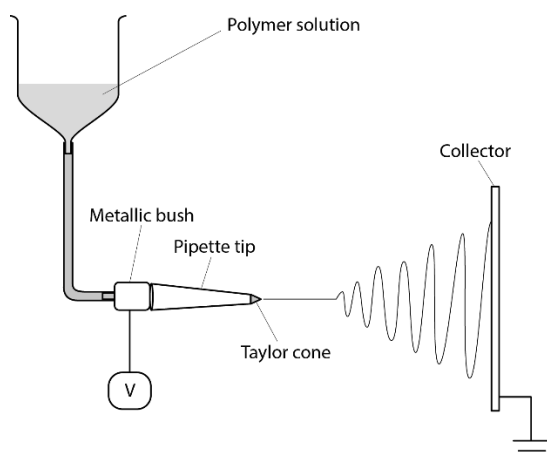


Figure 1. Schematic of the electrospinning set-up

## Processing and Fabrication of Advanced Materials XXV

Field-emission scanning electron microscopy (FE-SEM) was used to observe the electrospun PVOH. The electrospun samples were placed on carbon tabs and gold-coated for 180 s at 25 mA using a thermal evaporator (K975X coater, Quorum Technologies Ltd, United Kingdom). FE-SEM was performed with a JEOL 7000F FE-SEM (JEOL Ltd, Tokyo, Japan) using an accelerating voltage of 5 kV, probe current of 7 mA and working distance of 10 mm. For the collagen samples, a Jeol-5000 Benchtop SEM under high vacuum with 10 and 15 kV accelerating voltage was used.

The average fibre diameter and fibre diameter distribution of each sample was determined using digital image analysis (Electrospinz SEM Analyser™ software, Electrospinz Ltd, New Zealand). A minimum of 1800 measurements were obtained from each SEM micrograph of PVOH. Average diameters were obtained from 500–15000 diameter measurements for collagen solutions. A sufficiently high magnification (x50,000) micrograph was used for fibre diameter measurement to ensure that the most fibres were represented with a diameter of at least 20 pixels [7].

### Results and discussion

#### Physical properties of PVOH solutions

Polyvinyl alcohol (PVOH) polymers are hydrophilic linear copolymers of vinyl alcohol and vinyl acetate. This is because the chemical reaction used to produce polyvinyl alcohol (PVOH) involves the hydrolysis of vinyl acetate side groups (VA) with sodium hydroxide (NaOH) to give vinyl alcohol (VOH) and sodium acetate (NaOAc). Therefore, there are two aspects of PVOH structure that influence behaviour. These include the degree of polymerization (DP) (number of units combined in the polymer) characterised in the molecular weight (Mw) and the degree of hydrolysis (HD), which refers to the extent that PVA monomers have been converted to PVOH. As the HD decreases below 88%, PVOH is less crystalline, will dissolve more readily in water and its viscosity is less affected by storage time. This is due to an increasing number of acetate groups that disrupt inter- and intra- chain hydrogen bonding of such preparations. In contrast, fully hydrolysed PVOH is crystalline and requires heat input to disrupt the hydrogen bonding and bring about dissolution.

Consequently, partially hydrolyzed PVOH (i.e. 85–90%), as used in this study, is not expected to undergo gelation during cooling or during storage. This is particularly relevant in electrospinning because 1) it has been demonstrated that the inability to electrospin fully hydrolyzed PVOH is due to gelation [8] and 2) one cannot electrospin a polymer which is a gel, on the time scale of electrospinning. The physical properties of the PVOH solutions investigated in this study were analysed and compared to those already published for PVOH with various HD (%) and Mw (kDa).

#### *Surface tension*

One of the most common demonstrations of surface tension is water droplets forming as the flow of a water tap is reduced (and hence the liquid jet diameter). It reflects the action of the attractive intermolecular forces between the water molecules. At the liquid interface, these forces are mainly in the direction of the bulk. In contrast, at the air interface, molecules do not have the same atoms on all sides and thus cohere more strongly to those associated with them on the surface. The resulting force pulls the liquid towards the center and causes it to contract to form the smallest possible surface [9]. Surface tension can be measured by a tension meter as the maximum force per unit length acting on a plate or a ring before break-up of the fluid occurs.

For an electrospinning jet to develop, the surface charge of the polymer solution at the Taylor cone has to overcome the surface tension. In addition, after jet initiation has occurred and the polymer solution is being stretched, capillary break-up can occur if surface tension is high and polymer viscosity is low. Hence surface tension is an important parameter to control in the

electrospinning process.

The surface tension measurements of the PVOH solutions examined are shown in Figure 2 and compared with PVOH data from the literature. The surface tension of water, the solvent used in these studies, is 72 mN/m at 20 °C. It can be seen that at low polymer concentrations the surface tension decreased sharply from the value of the solvent and in the present study the surface tension continued to decrease, albeit at a lower rate, over the concentration range investigated. Most polymers act as surfactants when dissolved in a solvent, migrating from the bulk solution at the center of the pendant drop to the surface and adsorbing to the solvent-air interface. This results in decreased interaction between the solvent molecules at the surface thereby reducing the surface tension.

The  $M_w$  of a polymeric surfactant influences the surface tension as shown in Figure 2 when the data from the PVOH (85–90HD%, 118 kDa) (■) samples analyzed here are compared with the PVOH (88HD%, 127 kDa) [11] (x) data point. However, the stronger influence on surface tension for PVOH was shown as the degree of hydrolysis. The surface tension values were comparable for all samples at PVOH concentrations up to 2 wt% but as the concentration increased there was a greater difference between the surface tension of the PVOH solutions based on HD. The surface tension was lower for solutions based on partially hydrolysed PVOH than fully hydrolysed PVOH (Figure 2). A possible explanation for these results is that the fully hydrolysed PVOH had adopted an extended conformation and that affinity between the PVOH macromolecules and potential for physical gelation, pulled the polymer inside the droplets excluding water and pushing it towards the surface, leading to increased surface tension. In contrast, partially hydrolyzed PVOH contains more acetate groups and hence adopts a coiled conformation with an inner core composed of the hydrophobic vinyl acetate groups. As a result, a greater number of molecules can migrate to the surface, disrupting the water-film structure resulting in reduced surface tension with increasing polymer concentration.



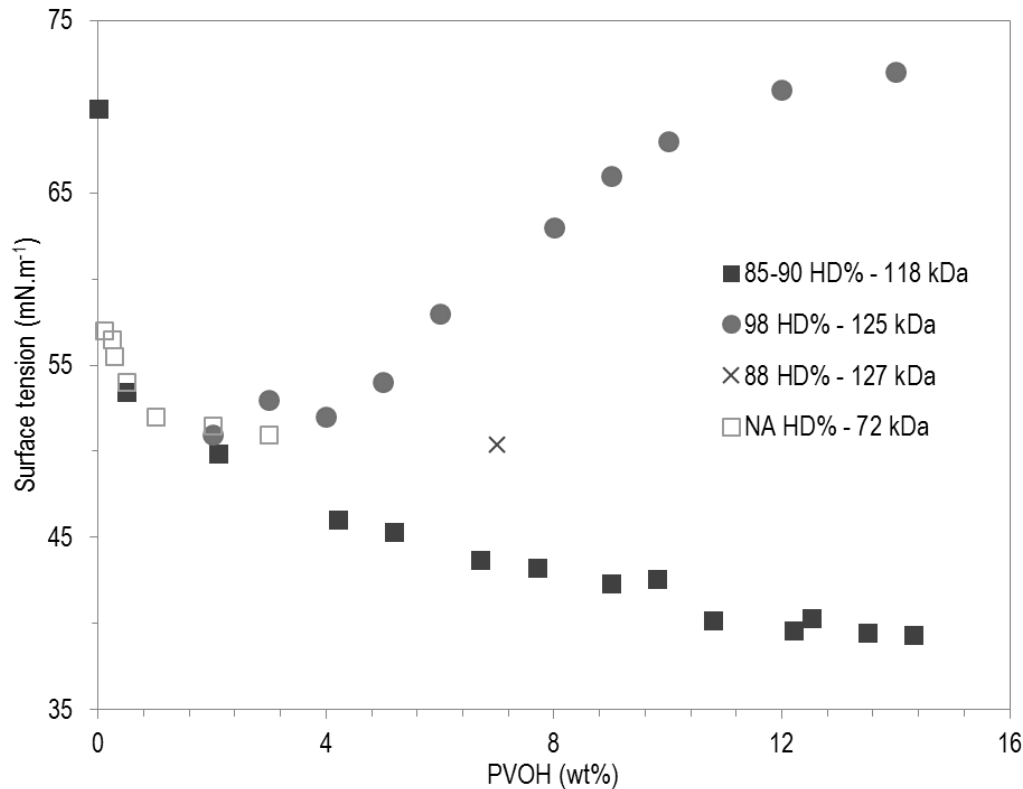


Figure 2. Surface tension as a function of PVOH concentration, degree of hydrolysis (HD) and molecular weight (MW) at 25°C for the present work (■); and after Rošić et al.[4] (●), Bhattacharya et al.[10], (□), and Peresin et al. [11](×).

### Electrical conductivity

The conductivity of a solution reflects the potential for bulk motion of the ions present and therefore is another important parameter in electrospinning. When a potential difference is applied across a volume of polymer solution as in the electrospinning process, an ion current that is proportional to the type and concentration of ions in the solution will flow.

Although PVOH is a non-electrolyte, electrical conductivity (greater than water) persists in PVOH solutions due to the presence of minor concentrations of salt (*e.g.* sodium acetate) remaining after manufacture. As shown in Figure 3, the conductivity of the PVOH solutions increased with increasing polymer concentration.

According to manufacturer Clariant [12], the electrical conductivity of 10% PVOH solutions is in the order of 0.1–0.7 mS.cm<sup>-1</sup> depending on ash content. Sekisui [13], producer of Selvol™ PVOH, report that the more hydrolyzed the PVOH, the higher the ash content. The ash content of fully hydrolyzed PVOH is 1.2%, while it is 0.9% for intermediate PVOH and 0.5–0.9% for partially hydrolyzed PVOH. This can be observed in Figure 3 where for a given concentration, the conductivity is greatest for 100% > 98% > 85–90% hydrolysis of the PVOH samples.

Differences observed between fully hydrolyzed PVOH (from [4]) and partially hydrolyzed PVOH (from the present study) can therefore be explained by differences in ash content.

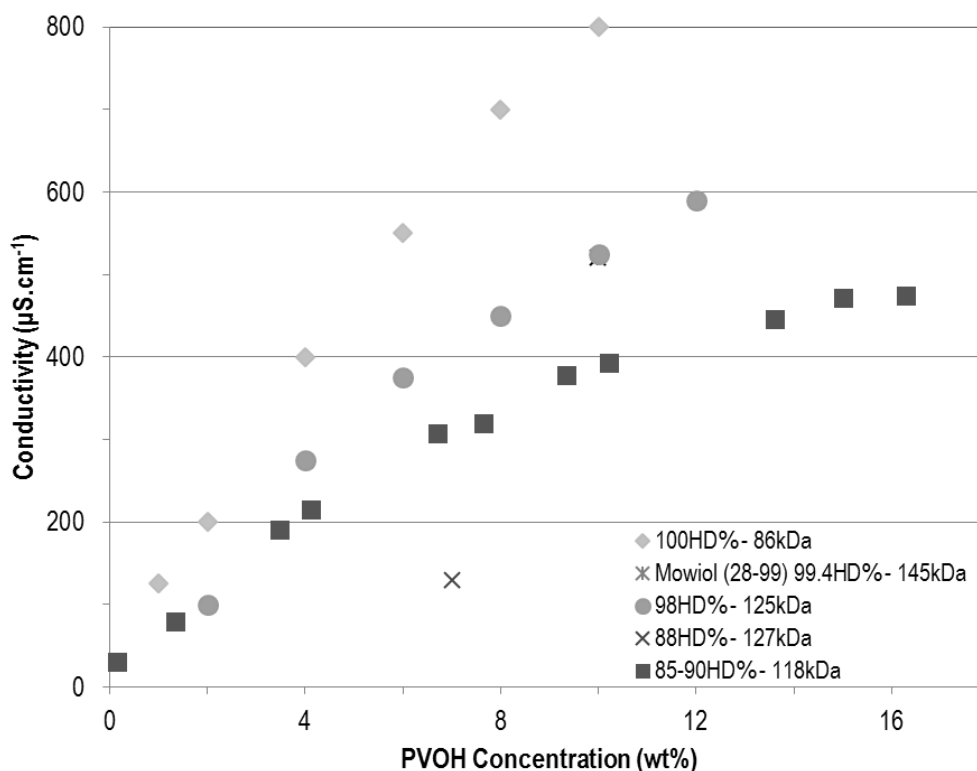


Figure 3. Electrical conductivity of PVOH solutions as a function of concentration and degree of hydrolysis (HD) at 25°C for the present work (■); and after Tang et al.[14] (×), Rošic et al. [4](●), Peresin et al. [15](✱), and Krise et al.[16] (◆).

### Viscosity

Although there is no clear definition of “entanglement” [17] it is often either simplified to be a property of long flexible polymers that entangle like spaghetti or more formally as a “persistent contact between mean path of the chains” [17]. It is widely accepted that for polymer electrospinning, entanglement significantly influences jet stabilisation and fibre formation [18]. In particular the minimum concentration for polymer electrospinning is often reported to be between  $C_e$  [19] and  $2.5 \times C_e$  [14] where the concentration of  $C_e$  (or entanglement concentration) is determined for each polymer. In a previous paper [20] we determined the entanglement concentration of the this PVOH material (85–90HD%, Mw 188kDa) to be  $C_e = 6.2$  wt%.

Although most common rheometers measure the shear viscosity of materials, i.e. the resistance of the material to shearing stress, the spinning process (such as melt spinning, wet spinning or electrospinning) exerts an extensional stress on the material.

According to Han *et al.*[12] and Helgeson *et al.*[13], the electrospinning jet consists of four distinct zones represented in Figure 4 : (i) A modified Taylor cone (the shape of the static Taylor cone is modified by the flow of the solution [14] and the electrical charge when the jet begins) with very low near-Newtonian flow and little extensional flow; (ii) a transition zone with very high elongational flow and shear rates of  $\sim 100$  to  $1000\text{ s}^{-1}$ ; (iii) a straight thin jet with a low pseudo-steady state elongational flow and shear rates  $\sim 20\text{ s}^{-1}$ ; and (iv) a jet that continues to accelerate and thin with negligible extensional stresses.

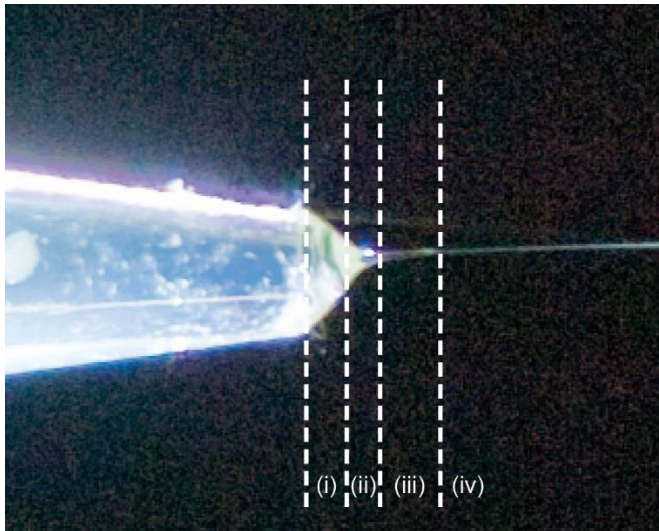


Figure 4. Electrospinning jet consisting of four distinct zones: (i) A modified Taylor cone with a very low near-Newtonian flow and little extensional flow; (ii) a transition zone with very high elongational flow and shear rates of  $\sim 100$  to  $1000\text{ s}^{-1}$ ; (iii) a straight thin jet with a low pseudo-steady state elongational flow and shear rates  $\sim 20\text{ s}^{-1}$ ; and (iv) a jet that continues to accelerate and thin with negligible extensional stresses. (Picture courtesy R. Lamberts, Plant & Food Research)

The resistance of a material to extensional stress is called extensional viscosity ( $\eta_e$ ). It can be measured by an extensional rheometer though it rarely reproduces spinning conditions. Although there is no direct relationship between shear viscosity and extensional viscosity at high strain rates, for low shear and extensional rates (where fluids are Newtonian) it was found experimentally by Trouton [21] that the extensional viscosity ( $\eta_e$ ) is three times the zero-shear viscosity ( $\eta_0$ , i.e. the shear viscosity at rates tending to zero).

As a consequence, it is assumed that the extensional viscosity within the Taylor cone (zone (i)) is  $\eta_e \sim 3 \cdot \eta_0$  since the shear rate is very small. Hence, zero-shear viscosity is used as an indicator for electrospinnability but is not representative of the whole process beyond the Taylor cone where strong extensional flow manifests.

The shear viscosity of PVOH solutions with different concentrations is presented in Figure 5.

Below the entanglement concentration, the solution exhibits Newtonian-like behaviour at the examined shear rates. The higher the concentration of PVOH above the entanglement concentration, the greater the amount of shear-thinning.

This is not in agreement with Rošic *et al.*[4] who reported that fully hydrolyzed PVOH with similar molecular weight (125kDa) exhibited Newtonian behaviour in the concentration range of 3 to 12 wt%. One could argue that at concentrations lower than 18 wt% and shear rates below 100 s<sup>-1</sup> (as presented by Rošic *et al.*[4] in supplementary data) PVOH solutions from the present work exhibit constant viscosity. However, shear-thinning behaviour is observed when extending the shear rate and concentration ranges to higher values. Furthermore, as explained earlier, the electrospinning of polymers is often attributed to entanglement effects, which implies that the PVOH solutions which electrospin must be non-Newtonian. Indeed, even Boger fluids (characterised by *nearly* constant viscosity) are not ideal Newtonian fluids. However, the discrepancy in observations could also be explained by differences in molecular conformation brought about by differences in HD. Hydrolyzed PVOH molecules are likely to exhibit less shear-thinning at higher shear rates than partially hydrolyzed PVOH due to the former containing more extended chains.

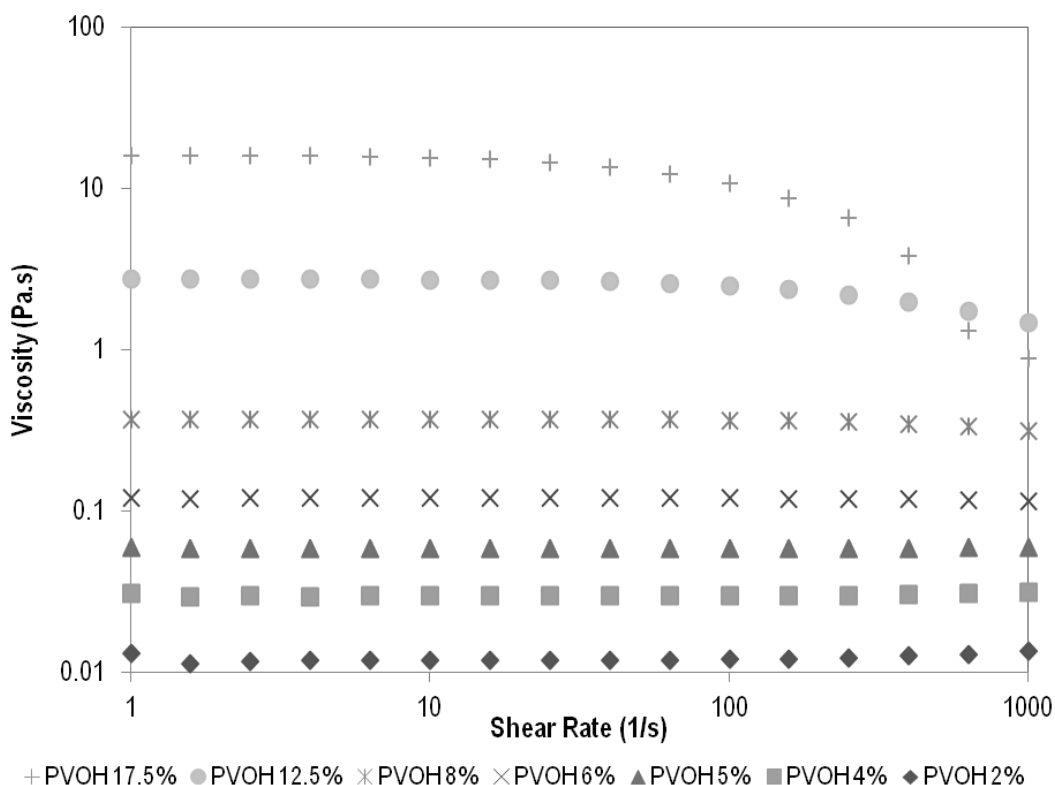


Figure 5. Shear viscosity of investigated PVOH for different concentrations at 25°C.

Despite discrepancies in flow behaviour, zero-shear viscosity values are consistent with previous studies. Figure 5 compares our results with a PVOH with similar molecular weight (118 kDa &

125kDa [4]) but different HD (88% Vs 98–99.8%) so that the effect of HD can be observed. For similar molecular weight and at a given concentration, higher HD% PVOH (■) has a more extended conformation than lower HD% PVOH (◆) giving less resistance to flow and lower viscosity.

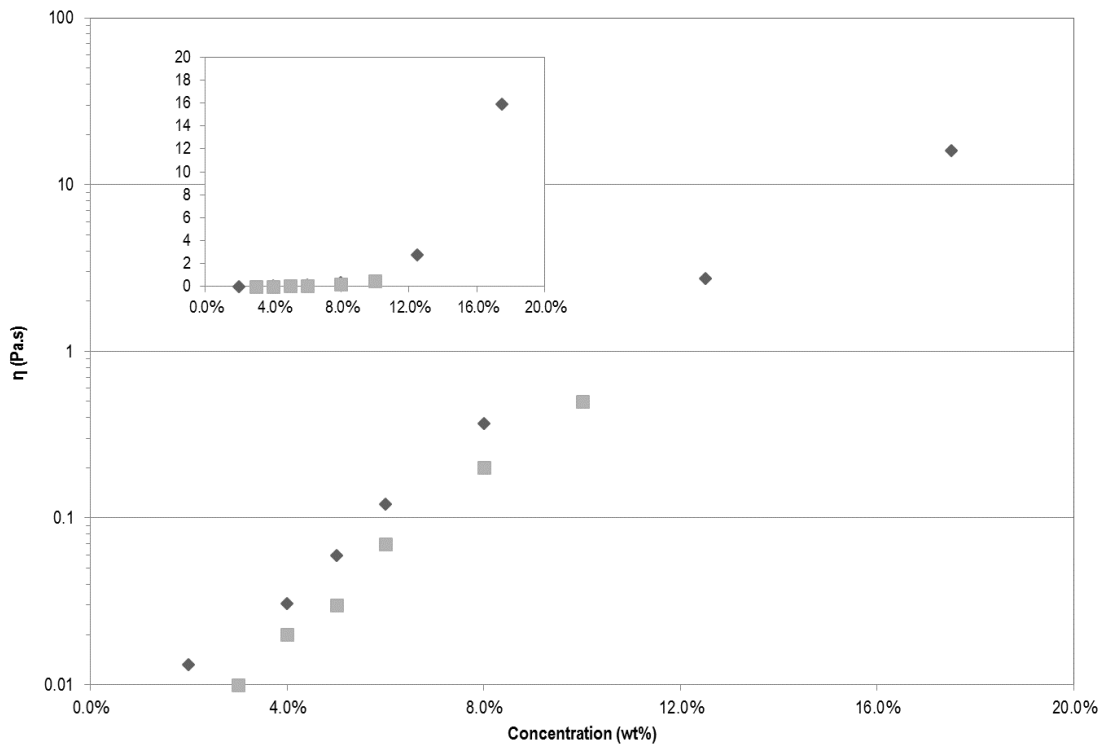


Figure 6. Zero-shear viscosity of PVOH for different concentrations at 25°C (◆) present study, (■) from Rošic et al.[4].

### Electrospinning

PVOH solutions with different concentrations and viscosity were electrospun using the same process parameters. Examples of the fibres developed are presented in Figure 7.

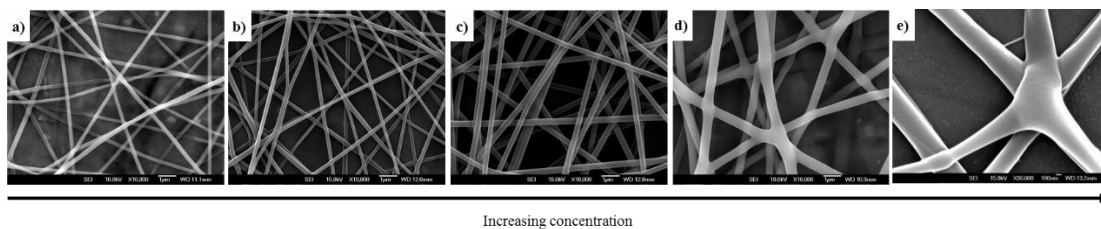


Figure 7. SEM micrographs of electrospun partially hydrolyzed PVOH solutions at different concentrations a) 6.7 wt%, b) 8 wt%, c)10 wt%, d)13.6 wt% and e)15.5 wt%.

Electrospinning at 6.7 wt% (ie. just above  $C_e$ ) and viscosity to 0.3Pa.s resulted in uniform thin fibres with some elongated beads. When the concentration was raised to 10 wt% and viscosity to 2Pa.s, the most uniform fibres were obtained. At 13.6 wt%, electrospun fibres were fused and in the micro-meter range in diameter. Electrospinning at 15.5% (which corresponds to Berry Number  $[\eta]C > 12$  [20]) and  $\eta_0 > 30$  Pa.s) resulted in the production of few fibres irregular in size and shape deposited in a whirling pattern, with bifurcations and fused intersections. Tao *et al.* reported the production of flat fibres with solutions at their Berry Number. These defects have previously been reported and were attributed to skin formation on the jet [22]. This is highly likely as with increased concentration, surface evaporation is faster.

### Designing an electrospinning window

We investigated a set of physical properties (surface tension, conductivity and viscosity) which render a polymer solution amenable to fibre formation and prepared a ternary plot using logarithmic scale for these solution properties. Using partially hydrolyzed PVOH (85–90%, BDH Chemicals) over a range of concentrations and the morphology of the fibres electrospun from these solutions, we identified the areas in the plot that showed the solution conditions that gave uniform fibres. This rendered an “electrospinning window” (Figure 8a), which described the specific physical parameter values that gave smooth regular nanofibres using a classic lab-scale electrospinning process with electric field of 2–3 kV/cm. The data from fully hydrolyzed PVOH as published by Rošić *et al.*[4] and Zhang *et al.* [23] was plotted on a similar format (Figure 8b) for comparison.

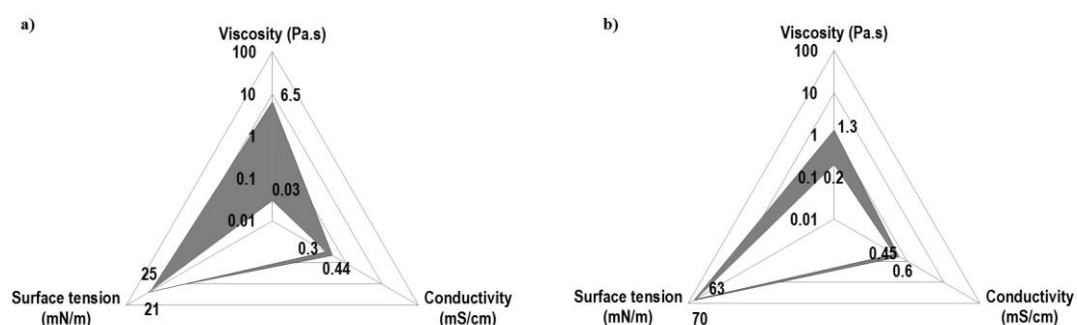


Figure 8. a) Ternary plot of surface tension, viscosity and conductivity using logarithmic scale showing, in shaded area, the solution properties of partially hydrolyzed (85–90%) PVOH, which gave uniform fibres with electrospinning, thus providing an “electrospinning window”. b) Published data from Rošić *et al.*[4] and Zhang *et al.*[23] (shaded area) plotted on a ternary diagram and showing solution properties of fully hydrolyzed (98–100%) PVOH solutions that gave uniform electrospun fibres.

There are notable differences between the “electrospinning windows” for the sample results plotted. In the study by Rošic et al.[4], the upper limiting concentration was identified as that above which nanofibres could no longer be obtained. In the present study, the upper limiting concentration was determined as that after which non-uniform fibres were obtained ( $C = 12.5$  wt%), as non-homogeneous fibres with sub-micron diameters were obtained at higher concentrations. It was observed that partially hydrolyzed PVOH could be electrospun from solutions which had lower values for each of the physical properties measured when compared with the fully hydrolysed PVOH samples. However, it is interesting to note that both partially and fully hydrolyzed PVOH could be electrospun from solutions with physical characteristics in the same order of magnitude: viscosity  $\sim 10^{-1}$ - $10^0$  Pa.s; surface tension  $\sim 10^1$  mN/m and conductivity  $\sim 10^{-1}$  mS/cm.

### *Effect of Conductivity*

Observations from fully hydrolyzed PVOH (Figure 8b) suggest that the electrospinning window for partially hydrolyzed PVOH (Figure 8a) could be extended with higher conductivity solutions. This is also supported when one considers the force balance of the electrospinning process represented in Figure 9.

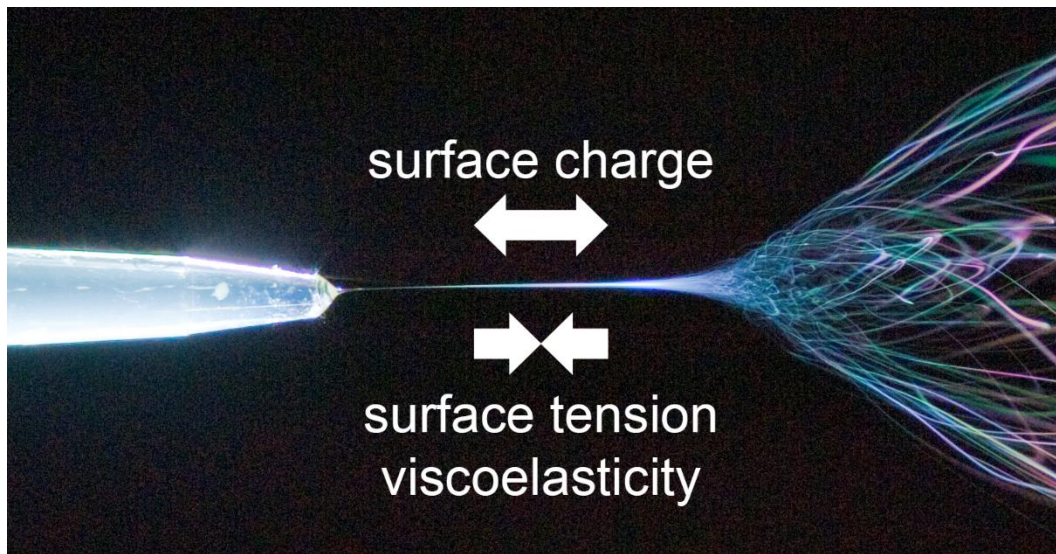


Figure 9. Representation of the force balance in the electrospinning process (Picture courtesy R. Lamberts, Plant & Food Research).

Supposedly, increasing the surface charge density should result in more stretching of the fibre. Hence small amounts of salts were added to the solution above the limiting concentration ( $C = 13.6\%$ ) and electrospun. As expected, higher conductivity increased the charge density of the jet and resulted in higher repulsive force which elongated it into finer and more homogeneous fibres. With the addition of salts, the average fibre diameter decreased from 526 nm to 470 nm, fibres were bead-free and not interconnected as observed previously. Similar results have been obtained from Zhang *et al.* [23] where 0.05 to 0.2% NaCl was added to a PVOH solution (7 wt%) and fibre diameter was reported to decreased from  $214 \pm 19$  nm to  $159 \pm 21$  nm. Stanger *et al.* [24, 25] studied the effect of higher NaCl concentrations (up to 0.5%) and observed that fibre diameter increased from 250 to 400 nm above solution conductivity of 1 mS/cm. Hence it seems that there is both a minimum conductivity (in order of 1  $\mu$ S/cm) necessary for the electrospinning to occur and a maximum limiting conductivity (in the order of 1 mS/cm), which limits the electrospinnability of a polymer solution.

### *Effect of Surface tension*

Surface tension plays an important role in electrospinning. At the beginning of the process, surface charge (brought about by the application of an electric field to a conductive solution) has to overcome surface tension and viscosity to initiate fibre formation. Following this, surface tension can be responsible for instabilities and consequent beading of the straight jet. Hence, intuitively, experimenters prefer lowering the surface tension of the polymer to electrospin at lower voltage and to limit bead formation. Yao *et al.*[25] studied the electrospinning of fully hydrolyzed PVOH (99.5HD%) and attributed its inability to electrospin to its high surface tension. Indeed, it was reported that surface tension of PVOH increases with degree of hydrolysis from 51 to 54 mN/m for 87 to 97HD% but sharply increased to 69 mN/m at for PVOH 99.5HD% near to the surface tension of water (72 mN/m). To facilitate the electrospinning of fully hydrolyzed PVOH, the authors used a small amount of Triton X-100 (0.03–1.5v/w%). They found that a minimum of 0.06v/w% was necessary for electrospinning to occur (and not spraying) but that the decrease in surface tension levelled off above 0.3v/w%. The solution electrospun particularly well with levels of Triton X-100 between 0.3 and 1.5v/w%. Unfortunately, only the contact angle values were given as a reflection of the decrease in surface tension. In our study, solutions with surface tension as low as 21 mN/m were electrospun, suggesting there is no minimum limiting value. However, one might imagine that if surface tension is too low, difficulties in obtaining a stable droplet at the tip of the spinneret might arise.



### *Effect of concentration and viscosity*

There is obviously a minimum polymer concentration for electrospinning to occur, corresponding to a sufficient level of elasticity in the polymer solution often brought about by entanglement effects as described elsewhere [8, 18, 19, 26, 27] or cohesive forces. Zhang *et al.* [23] reported the electrospinning of low molecular weight PVOH with viscosity as low as 0.1 Pa.s.

However, there is also an upper limiting concentration for electrospinning [20]. Most authors [4, 28, 29] relate it to the high viscosity of the polymer because at high concentrations surface tension is low and conductivity is high. Hence, another way to widen the “electrospinning window” of PVOH would be to decrease viscosity.

This strategy has been investigated by some authors [30, 31] who have applied vibration technology to concentrated polymer solutions for electrospinning as a means to obtain finer fibres at higher polymer concentrations or to use lower voltage. This approach was based on the belief that vibrating forces applied to concentrated and entangled polymer solutions or melts weaken the Van Der Waals forces connecting the macromolecules, relaxing the entangled networks and reducing the viscous force between macromolecules resulting in lower viscosity [32]. The concept was demonstrated using on polyacrylonitrile (PAN)/DMF solution [31] and was patented [30]. More recently [20], a new setup which shears the polymer just before electrospinning was proposed and allowed electrospinning PVOH with concentration up to 30 wt%. Finally, Liu *et al.* [33] reported the use of hydrazine monochloride (HMC) as a viscosity reducer for electrospinning high molecular weight PVOH.

Based on the data from the literature, the present study and consideration of the magnitude of the various physical parameters (increased or decreased conductivity, surface tension and viscosity), the following “electrospinning window” (Figure 10) is proposed for PVOH electrospun at 2–3 kV/cm and at a flow rate giving a stabilised droplet.

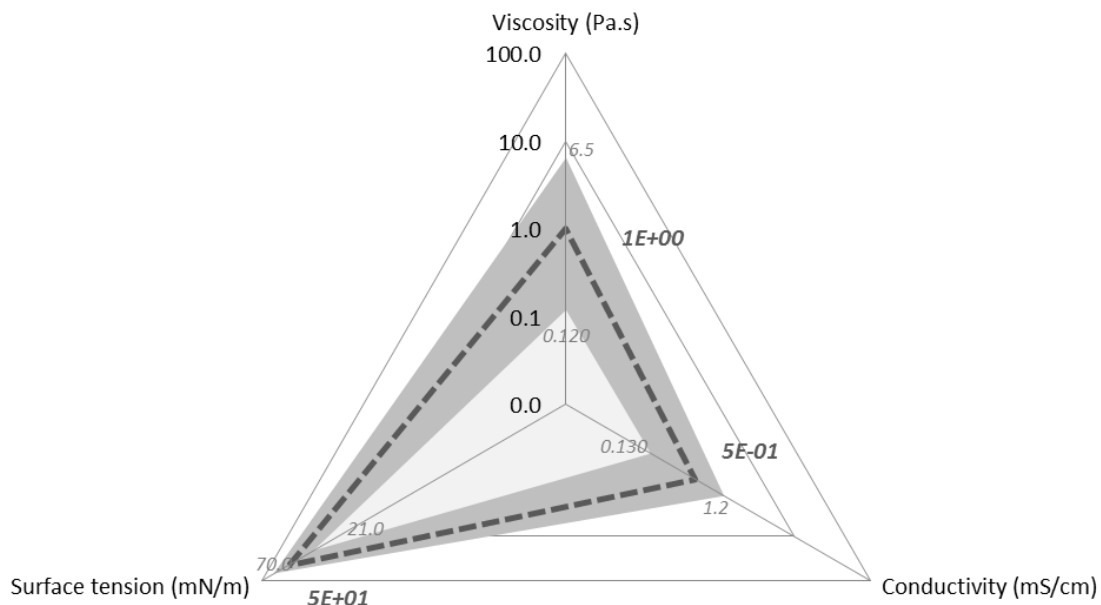


Figure 10. A proposed “electrospinning window” for achieving uniform fibres from solutions of PVOH which have the physical property values outlined by the shaded area. The dotted line represents the ideal target values.

These values are in good agreement with physical parameters from poly (ethylene oxide) (PEO), another polymer used for modelling the electrospinning process [34, 35] with solution properties of surface tension ( $6 \cdot 10^1 \text{ mN/m}$ ), Conductivity ( $0 \sim 10^1 - 10^2 \mu\text{S/cm}$ ) and Viscosity ( $0 \sim 10^0 \text{ Pa.s}$ ). We believe this window can be used for designing the physical properties of solutions of other polymers, especially those of biological origin which are difficult to electrospin due to one of the physical parameters being too high. Indeed, a number of biopolymers act as polyelectrolytes, surfactants and/or have high viscosity at low concentration. The applicability of this defined “electrospinning window” to biopolymers was then verified in a case study using denatured whole chain collagen (DWCC) electrospun from two different acids (acetic and citric).

**Applicability of the proposed “electrospinning window” – Case study: denatured whole chain marine collagen in organic acids**

Collagen samples with mass fraction of collagen and acid (Table 1) as illustrated in the ternary diagram (Figure 10) were prepared. The solutions were electrospun and rendered bead-on-string structures, nanofibres, macrofibres or did not spin. Above 0.40 collagen mass fraction, electrospinning was not possible because the viscosity of the solutions were so high that they would not flow into the electrospinning machine. Surface tension measurements were also unreliable at these concentrations.

Table 1. Mass fraction composition of the marine collagen samples (coded A1 to A8 and C1 to C4) used to test the “electrospinning window”.  $F_{DWC}$  is the mass fraction of denatured whole chain marine collagen,  $F_{AcOH}$  and  $F_{CA}$  are the acetic acid and citric acid mass fraction of the sample respectively and  $F_{H_2O}$  is the mass fraction of water so that  $F_{DWC}+F_{acid}+F_{H_2O}=1$ . The last column reports the result of electrospinning these samples at 3 kV/cm.

Code	$F_{DWC}$	$F_{AcOH}$	$F_{H_2O}$	Electrospinning morphology
A1	0.1	0.05	0.85	Beads
A2	0.1	0.3	0.6	Beads
A3	0.1	0.6	0.3	Nanofibres – Wet and fused
A4	0.17	0.08	0.75	Nanofibres
A5	0.17	0.75	0.08	Nanofibres
A6	0.2	0.7	0.1	Microfibres (>1000 nm)
A7	0.2	0.3	0.5	Microfibres (>1000 nm)
A8	0.3	0.5	0.2	Microfibres (>1000 nm)
	$F_{DWC}$	$F_{CA}$	$F_{H_2O}$	Electrospinning
C1	0.1	0.1	0.8	Bead-on-string / wet
C2	0.2	0.1	0.7	Nanofibres
C3	0.25	0.2	0.55	Microfibres (>1000 nm)
C4	0.3	0.15	0.55	Non electrospinning

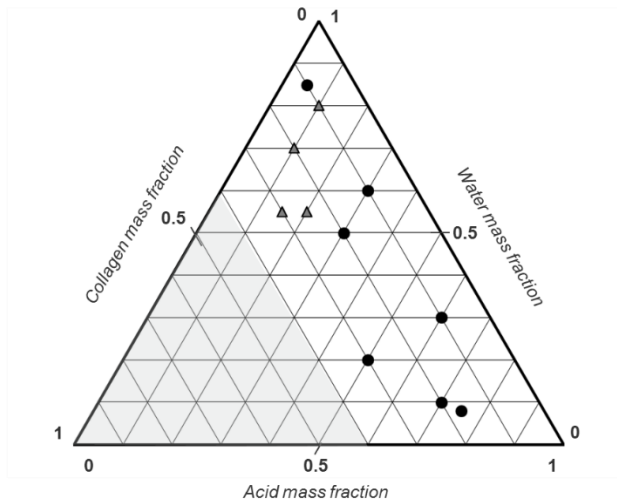


Figure 11. Ternary diagram of denatured whole chain collagen/acid/water showing the distribution of the solutions prepared in acetic acid (●) and citric acid (▲).

The properties of these collagen solutions were measured and plotted on the “electrospinning window” as presented in Figure 12. The samples which rendered beads are plotted in orange and are shown to fall outside the window on the conductivity side, with only one sample falling low on the viscosity side. The samples which resulted in microfibres are plotted in blue and these have viscosity values that are above the “electrospinning window” but enough conductivity to pull the polymer into fibres. A similar plot (bolder most outer-line on the viscosity side) was obtained for the sample which did not electrospin (C4) and which had equally high viscosity but relatively lower conductivity.

The samples which electrospun uniform fibres in the nanometer range are plotted in green and the solution properties of these samples are all within the boundaries defined by the “electrospinning window” model presented in this work. These results show the applicability of the proposed “electrospinning window” defining solution properties for collagen electrospinning and potentially for other biopolymers.

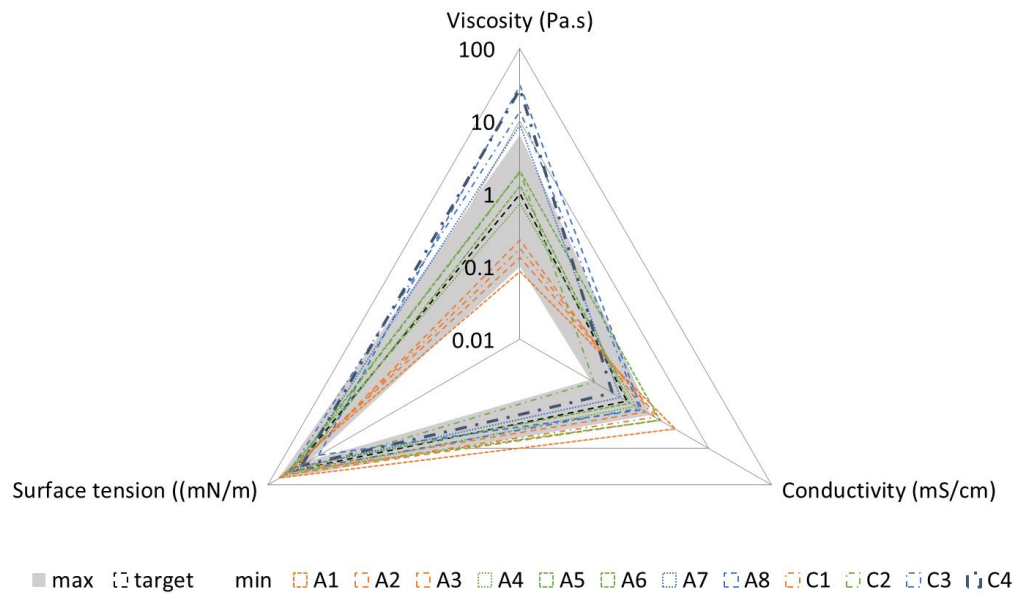


Figure 12. The measured properties for a range of denatured whole chain collagen solutions prepared in either acetic or citric acid plotted on a ternary diagram with logarithmic scale and compared with the “electrospinning window” (grey shaded area) proposed from PVOH data. The sample codes define the mass fractions of each of the samples as identified in Table 1.

## Conclusions

The physical properties of aqueous poly(vinyl alcohol) solutions from the literature and experiments were used to define an “electrospinnability window”. Target values for solution electrospinning under classic conditions (stable droplet and electric field 2–3 kV/cm) were estimated to be viscosity 1Pa.s, conductivity below 1 mS/cm and surface tension lower than 54 mN/m.

Solutions of denatured whole chain collagen in acetic acid and in citric acid were prepared to different ratios, electrospun and compared with the proposed map.

The results show that the “electrospinnability window” model has the potential to provide a processing map that might aid the design of electrospinnable biopolymer solutions.

## References

1. Tucker, N., et al. *Journal of Engineered Fibres and Fabrics*, 2012. **7**(Special Edition).
2. Doshi, J. and D.H. Reneker. *Journal of Electrostatics*, 1995. **35**(2–3): p. 151-160.
3. DeMerlis, C.C. and D.R. Schoneker. *Food and Chemical Toxicology*, 2003. **41**(3): p. 319-326.
4. Rošić, R., et al. *European Polymer Journal*, 2013. **49**(2): p. 290-298.
5. Hofman, K., et al. *Journal of Materials Science*, 2012. **47**(3): p. 1148-1155.
6. LeCorre-Bordes, D., P. Jaksons, and K. Hofman. *Journal of Materials Science*, 2016.
7. Stanger, J.J., et al. *Polymer Testing*, 2014. **40**: p. 4-12.
8. Shenoy, S.L., W.D. Bates, and G. Wnek. *Polymer*, 2005. **46**(21): p. 8990-9004.
9. Database, P.P. 2015 [cited 2016 November 2016]; Available from: <http://polymerdatabase.com/polymer%20physics/InterfacialTension.html>.
10. Bhattacharya, A. and P. Ray. *Journal of Applied Polymer Science*, 2004. **93**(1): p. 122-130.
11. Peresin, M.S., et al. *Biomacromolecules*, 2010. **11**(3): p. 674-681.
12. Clariant GmbH, D.C. 1999, Division CP BU Polyvinyl Alcohol / Polyvinyl Butyral Marketing. p. 54(D15).
13. Chemicals *Selvol* 2013; Available from: <http://www.sekisuis-sc.com/products/selvole/index.html>.
14. Tang, C., et al.. *Macromolecules*, 2010. **43**(2): p. 630-637.
15. Peresin, M.S., et al. *Biomacromolecules*, 2010. **11**(9): p. 2471-2477.
16. Krise, K.M., et al. *The Journal of Physical Chemistry B*, 2011. **115**(12): p. 2759-2764.
17. Likhtman, A.E. and M. Ponmurugan. *Macromolecules*, 2014. **47**(4): p. 1470-1481.
18. Shenoy, S.L., et al. *Polymer*, 2005. **46**(10): p. 3372-3384.
19. McKee, M.G., et al. *Macromolecules*, 2004. **37**(5): p. 1760-1767.
20. LeCorre-Bordes, D., et al. *Journal of Materials Science*, 2016. **51**(14): p. 6686-6696.
21. Wisniak, J. *The Chemical Educator*, 2001. **6**(1): p. 55-61.
22. Koombhongse, S., W. Liu, and D.H. Reneker. *Journal of Polymer Science Part B: Polymer Physics*, 2001. **39**(21): p. 2598-2606.
23. Zhang, C., et al. *European Polymer Journal*, 2005. **41**(3): p. 423-432.
24. Stanger, J.J., et al. *AIP Conference Proceedings*, 2009. **1151**(1): p. 118-122.
25. Yao, L., et al. *Chemistry of Materials*, 2003. **15**(9): p. 1860-1864.
26. McKee, M.G., C.L. Elkins, and T.E. Long. *Polymer*, 2004. **45**(26): p. 8705-8715.
27. Yu, J.H., S.V. Fridrikh, and G.C. Rutledge. *Polymer*, 2006. **47**(13): p. 4789-4797.
28. Kanjanapongkul, K., S. Wongsasulak, and T. YooviHDya. *Journal of Applied Polymer Science*, 2010. **118**(3): p. 1821-1829.

## Processing and Fabrication of Advanced Materials XXV

29. Kriegel, C., et al. Crit. Rev. Food Sci. Nutr., 2008. **48**(Copyright (C) 2012 American Chemical Society (ACS). All Rights Reserved.): p. 775-797.
30. Wan, Y.Q., et al. 2004: China.
31. Wan, Y.-Q., et al. Materials Letters, 2006. **60**(27): p. 3296-3300.
32. He, J.-H., Y.-Q. Wan, and J.-Y. Yu. International Journal of Nonlinear Sciences and Numerical Simulation. 2004. p. 253.
33. Liu, F., et al. Sen'i Gakkaishi, 2012. **28**(3): p. 49-54.
34. Han, T., A.L. Yarin, and D.H. Reneker. Polymer, 2008. **49**(6): p. 1651-1658.
35. Helgeson, M.E., et al. Polymer, 2008. **49**(12): p. 2924-2936.